Journal of Organometallic Chemistry, 341 (1988) 39–51
Elsevier Sequoia S.A., Lausanne – Printed in The Netherlands

Organo-magnesium reagents: the crystal structures of [Mg(anthracene)$(THF)_3$] and [Mg(triphenylmethyl)Br$(OEt_2)_2$] *

Lutz M. Engelhardt, Stephen Harvey, Colin L. Raston *, and Allan H. White

Department of Physical and Inorganic Chemistry, The University of Western Australia, Nedlands, W.A. 6009 (Australia)

(Received August 15th, 1987)

Abstract

[Mg(anthracene)$(THF)_3$] (**1**), (THF = tetrahydrofuran), is monomeric in the solid state; the metal is bound to the C(9) and C(10) centres with $\bar{r}$(Mg–C) 2.30 Å, and the $[anthracene]^{2-}$ ligand folded along the C(9)–C(10) vector with a mean angle of 28.6°. [Mg$(CPh_3)Br(OEt_2)_2$] (**4**) is also monomeric; the metal centre is four-coordinate, bound only to the *ipso*-carbon of the carbanion, r(Mg–C) 2.25(1) Å. Reaction of **1** or elemental magnesium with $BrCPh_3$ in THF or addition of THF to **4**, yields a red solid of the Grignard reagent containing some paramagnetic species.

[Mg(anthracene)$(THF)_3$], (**1**) (THF = tetrahydrofuran) has unusual properties in its ability to react as a di-nucleophile [1,2] and as a source of atomic magnesium [1, 3–5] (e.g. in the formation of benzylic type Grignard reagents, eq. 1, $x = 2$ [4]).

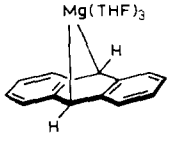

(1)

$$+ \quad (Aryl)_{3-x}CH_xX \xrightarrow[-C_{14}H_{10}]{+THF} (Aryl)_{3-x}CH_xMgX(THF)_n \qquad (1)$$

(X = Cl or Br)

On the basis of ^{13}C NMR data [6] and the structures of magnesium complexes of substituted anthracenes [5,7,8], compound **1** has been assigned a monomeric structure with the magnesium bridging the C(9) and C(10) carbon centres [7]. However, without structural data and/or molecular weight measurements, an oligomeric structure cannot be ruled out, particularly in the light of the structures of the

* Dedicated to Professor Colin Eaborn in recognition of his contribution to organometallic chemistry.

0022-328X/88/$03.50

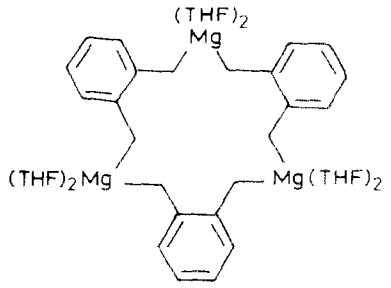

(2)

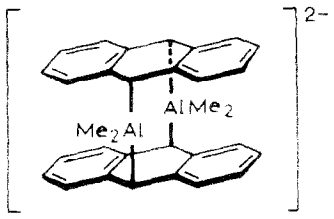

(3)

magnesium [9] and aluminium [10] complexes (**2** and **3**). To settle this, the X-ray structure of **1** has been determined and the results reported herein.

Also reported are the syntheses of the Grignard reagent of $BrCPh_3$ from **1** (eq. 1, $x = 0$, X = Br) or elemental magnesium in THF and the X-ray structure of the Grignard reagent of the same organic halide, $[Mg(CPh_3)Br(OEt_2)_2]$ (**4**) but prepared from elemental magnesium in diethyl ether/benzene. These compounds are of interest for the type of interaction of the carbanion to the metal centre, and whether it differs from the cases where the *ipso*-carbon bears only two phenyl groups, (compound **1**), or is a simple benzylic compound, such as **2** [9]. Surprisingly, there are only a few structurally authenticated metal complexes containing the triphenylmethyl ligand, viz. (i) $[M(CPh_3)(TMEDA)]$ (TMEDA = *N,N,N′,N′*-tetramethyl-1,2-diaminoethane; M = Li [11] or Na [12]), which have contact ion-pair structures, each metal centre bound to a trigonal planar *ipso*-carbon and three or four other carbon atoms respectively, shown below for the lithium derivative **5**, and (ii) a tin complex where the metal is σ-bonded to the *ipso*-carbon [13].

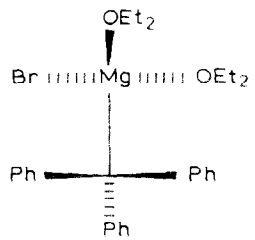

(4)

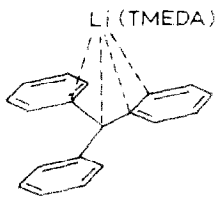

(5)

Preparation and structural studies

Orange crystals of **1** formed over two months from an undisturbed THF solution of anthracene, ca. 0.1 *M*, in contact with an excess magnesium previously activated with 1,2-dibromoethane in THF and washed with fresh THF. This method of obtaining crystals for X-ray diffraction studies was recently successful for $[Mg_2(C_{12}H_8N_2)Br_2(THF)_6]$. $[MgBr_2(THF)_4]$ containing the dianion of phenazine [14], which is isoelectronic with the dianion of anthracene.

Compound **1** crystallizes in space group $C2/c$ with cell volume 4700(4) Å^3; an unsuccessful attempt at determining the structure was based on data derived for a triclinic cell of similar cell volume, 4669 Å^3, with one of the cell angles suspiciously close to 90° [15]. The asymmetric unit is comprised of two discrete monomeric metallabicyclic species in which the metal centres are bound by the central carbons of the formally [anthracene]$^{2-}$ ligand ($\bar{r}$(Mg–C) 2.30 Å; cf. $\bar{r}$(Mg-adjacent ring carbons) 2.7_3 Å), and three THF moieties. Thus, the metal centres are five-coordinate (Fig. 1) and are similar to those in the structure of the corresponding 1,4-dimethylanthracene complex, [Mg(1,4-$Me_2C_{14}H_8$)$(THF)_3$] (**6**) [7]. This contrasts with π-bonding in the related complex [Mg(η^4-*cis*-PhCHCHCHCHPh)$(THF)_3$] (r(Mg–C_{Ph}) 2.29 Å; r(Mg–C_H) 2.54 Å) [16]. Complex **1** is like other magnesium anthracene complexes, **6** [7], [Mg(9,10-bis(trimethylsilyl)anthracene)$(THF)_2$] (**1**) [5,8], or [Mg(9,10-bis(trimethylsilyl)anthracene)(TMEDA)] (**8**) [5] in both the metal-to-ligand interaction and the folding of the anthracene group along the vector between the central carbons. In **1**, the angle between the two phenyl planes of each [anthracene]$^{2-}$ ligand is 26.6° for molecule A and 30.6° for molecule B.

Orientation of the ligands with respect to 'Mg(anthracene)' and torsion along Mg–O bonds are the only major differences in the two independent molecules (Fig. 1). Geometries are identical within experimental error, and do not differ significantly from those of compound **6** [7], despite the presence of electron-releasing methyl groups; e.g. r(Mg–C) 2.30 in **1** and 2.32 Å in (**6**), mean angle C–Mg–C 71.4 in **1** and 72.6° in **6**. In the silylated anthracene complexes **7** [5,8] and **8** [5], the Mg–C distances are much shorter, 2.22_3 and 2.21_9 Å respectively, and the C–Mg–C angles more acute, 78.9(3)° and 78.1(3)°, respectively. This could arise from the metal centres in **1** and **8** possessing fewer co-ligands, most likely a consequence of otherwise steric buttressing from the silyl groups, and/or polarization and concentration of charge by silicon on C(9) and C(10) [17]. The Mg–O distances in **1** are unexceptional for five-coordinate magnesium bearing three THF ligands [7,16].

Folding of the [anthracene]$^{2-}$ ligand, and the presence of polarized covalent bonds involving sp^3 carbon centres (supported by ^{13}C NMR data) [6] in anthracenemagnesium complexes, contrasts with an almost planar dianion (and thus sp^2 central carbon atoms) in an anthracenelithium complex, [Li(anthracene)$(TMEDA)_2$] [18], where the bonding is essentially ionic. Loss of aromatic character on reduction of anthracene, and concomitant magnesium-to-carbon bond formation in **1**, is reflected in elongation of the C(9) and C(10) to adjacent carbon atom distances, 1.47 Å, as for **6** [7], 7 and **8** [5,8]. In the above lithium complex, conjugation in the dianion is manifested in shorter distances, 1.42_7 Å [18].

Compound **4** was prepared by the reaction of $BrCPh_3$ with activated magnesium in diethyl ether/benzene, according to the literature procedure [19]. Suitable crystals for an X-ray structure determination were obtained over several days using magnesium ribbon. Reaction of the bromide with magnesium in THF yielded a red, sparingly THF soluble solid, **9**, containing paramagnetic species (broad singlet, $g = 2.0031$). Analytical data were variable, but the ratio of $[CPh_3]^-$ to THF was consistently 1/3 (established from ^{1}H NMR spectra of the CCl_4 decomposition mixture). The same paramagnetic solid formed using **1** as a source of magnesium (eq. 1) and on addition of THF to the diethyl etherate (**4**).

In diethyl ether, compound **4** does not absorb visible radiation [20], which is consistent with a σ-*ipso*-carbon-to-magnesium contact (see below). In contrast, the

(*Continued on p. 44*)

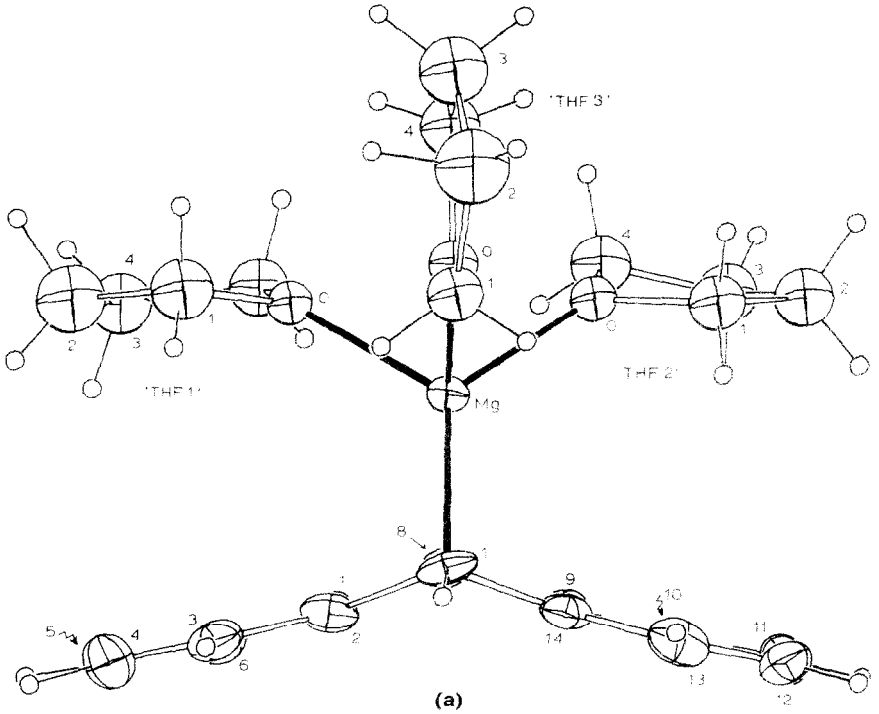

(a)

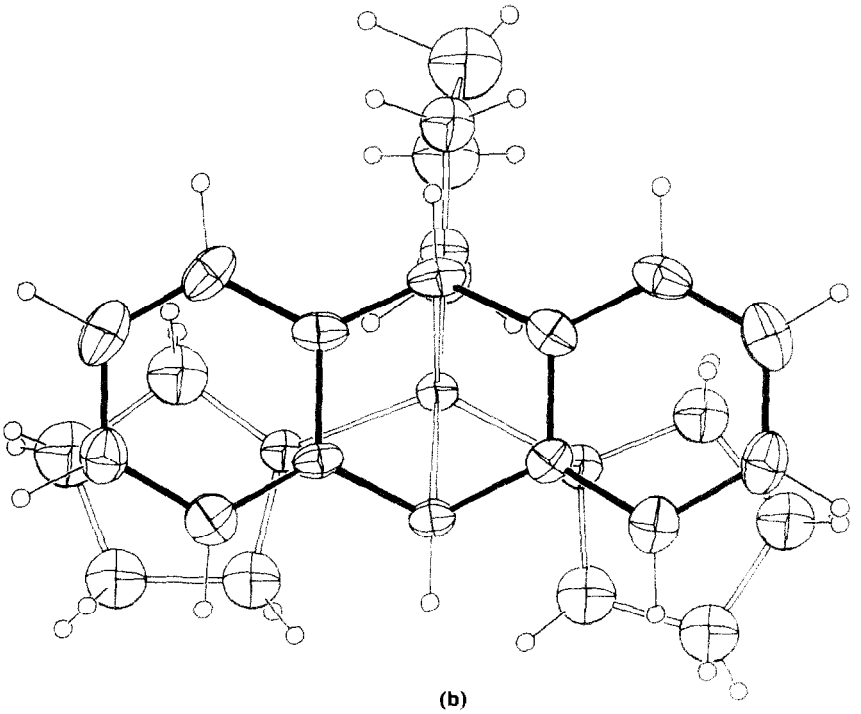

(b)

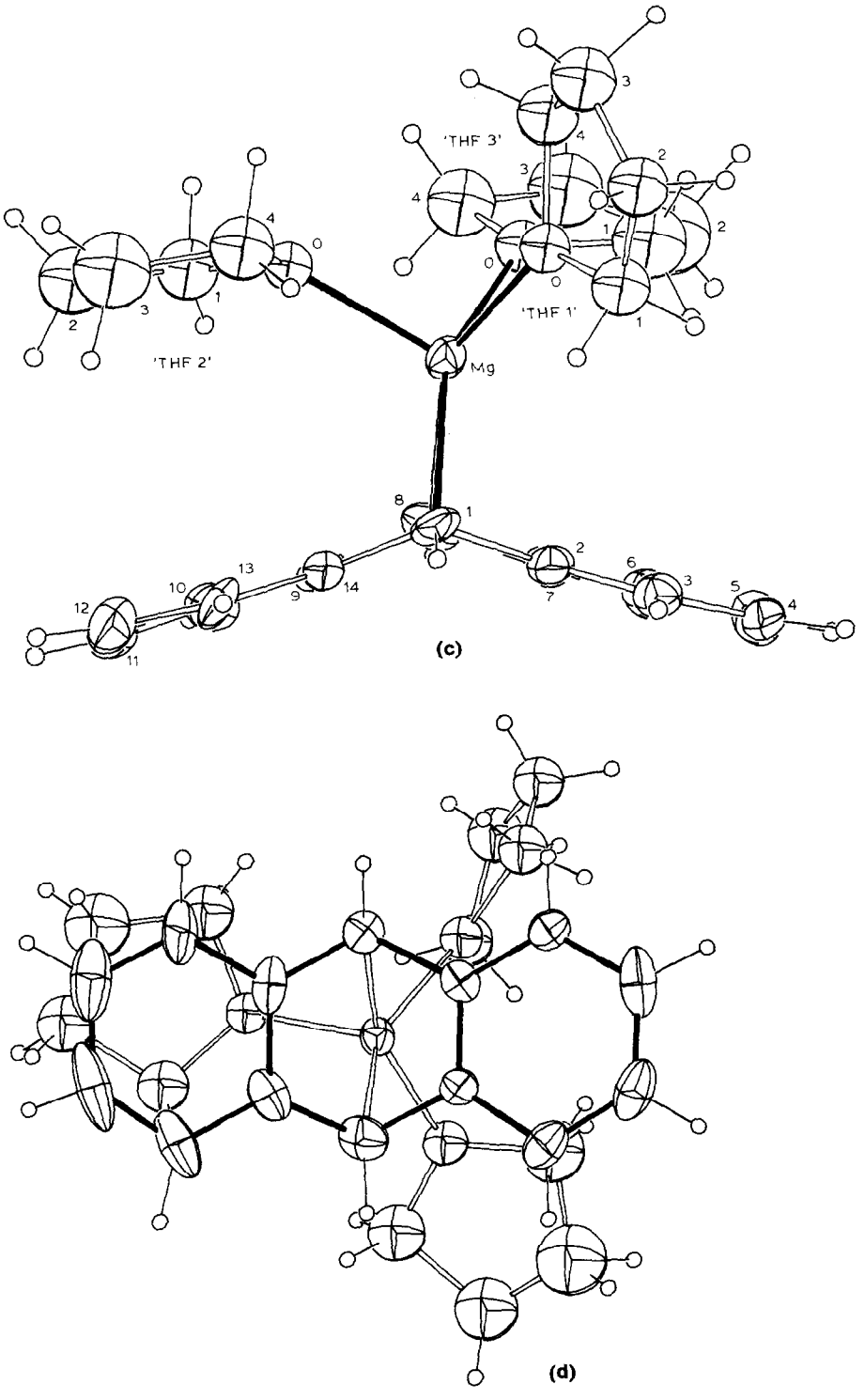

Fig. 1. Projections of the two crystallographic independent molecules in [Mg(anthracene)$(THF)_3$] (**1**); (a) and (b) correspond to molecule A and (c) and (d) to molecule B. 20% thermal ellipsoids for non-hydrogen atoms are shown; hydrogen atoms have arbitrary radii of 0.1 Å.

alkali metal complexes of $[CPh_3]^-$ absorb strongly, e.g. at 450 and 480 nm, respectively, for lithium and potassium complexes. They have been assigned contact ion-pair structures [21], and presumably have metal polyhapto-carbanion interactions, like in [M(TMEDA)(CPh_3)] (M = Li [11] or Na [12]) with a trigonal-planar *ipso*-carbon and extensive delocalization of charge. The same alkali metal complexes in THF have solvent separated structures, with λ_{max} ca. 500 nm [21]. In general, the greater the ionic character, the larger λ_{max}.

What is the nature of **9**? Tetrahydrofuran solutions absorb at 410 and 500 nm to approximately the same degree. This compared with a maximum at 500 nm and a shoulder at 432 nm for **4** in a mixture of diethyl ether and tris(dimethylamino)phosphine (HMPT) [22], the 500 nm band matching that of solvent-separated ion-pairs in the above alkali metal complexes. However, the 500 nm band for **9** appears to arise from trace amounts of paramagnetic species, not $[CPh_3]^\cdot$, although this is present since THF solutions gave EPR spectra with resolved hyperfine coupling very similar to that reported for the same radical in other solvents, albeit only at high dilution [23]. We conclude that the concentration of $[CPh_3]^\cdot$ is much higher than that of the species responsible for the 500 nm band. Exposure of solutions of **9** to oxygen resulted in rapid change in colour from deep red to yellow, and concomitant loss of the 500 nm peak, the peak at 410 nm being unperturbed, and quenching of the radicals (EPR) to $(OCPh_3)_2$ in the case of $[CPh_3]^\cdot$ [24]. This had negligible effect on the activity of the solutions (acid quenching and back titration with base) which behaved as Grignard reagents in yielding $DCPh_3$ as the major product when treated with DCl/D_2O. The extinction coefficient of the 410 nm band is ca. 250 l mol^{-1} cm^{-1}. That of the broad 500 nm band could not be determined because of the low concentration of the responsible species, but it must be very high, perhaps comparable to that of the carbanion, $[CPh_3]^-$, ca. 20000 l mol^{-1} cm^{-1}. This would mask the 513 nm band for $[CPh_3]^\cdot$ which has a low extinction coefficient, ca. 139 l mol^{-1} cm^{-1} [25].

Thus, **9** appears to be mainly the Grignard reagent $[Mg(CPh_3)Br(THF)_3]$, although it could not be isolated analytically pure. The band at 410 nm is attributed to this species possessing some delocalization of charge, less than in the above contact ion-pair structures, and we propose an interaction of magnesium-to-carbanion similar to that in **4**, but with slightly more ionic character brought about by the greater solvation of the metal centre. Its noteworthy that $[CPh_3]^\cdot$ crystallizes as the diamagnetic Gomberg dimer (eq. 2) [24], so it is unlikely that the radical in the solid of **9** is $[CPh_3]^\cdot$.

$$2\,[CPh_3]^\cdot \rightleftharpoons \quad \text{(Ph, H, Ph, CPh}_3\text{)} \qquad (2)$$

The 500 nm band for **9** in THF does not match that of $[CPh_3]^\cdot$ in THF (λ_{max} 513 nm, as in OEt_2 [25]) and solutions of **9** are deep red, whereas those of $[CPh_3]^\cdot$ are red/orange. We propose that the species responsible for this band is the radical anion **10**, which is formed irreversibly by combination of $[CPh_3]^-$ and $[CPh_3]^\cdot$ and/or electron transfer to the preformed Gomberg dimer (eq. 4), and that $[CPh_3]^\cdot$ present (EPR) comes from dissociation of the dimer present in the solid. The radical anion is not formed on the addition of a THF solution of the Grignard reagent, previously quenched with dioxygen to remove paramagnetic species ($[CPh_3]^\cdot$ and

10), to a THF solution of $[CPh_3]^{\cdot}$ (Gomberg dimer and THF, eq. 2). Formation of the same radical anion on treating **4** with THF could arise from dissociation of traces of the dimer (eq. 2), followed by association with Grignard species.

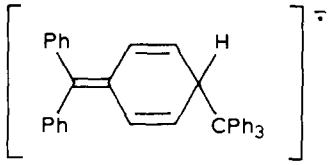

(**10**)

Material containing a greater amount of the radical anion **10** is generated on treating magnesium with an excess of $BrCPh_3$, although only up to a ratio of 2/1. Above this, only the simple triphenylmethyl radical is formed (eq. 3). Its THF solutions also react with dioxygen to form yellow solutions containing Grignard species.

$$2\ BrCPh_3 \xrightarrow{Mg/THF} 2\ [CPh_3]^{\cdot} + MgBr_2(THF)_4 \qquad (3)$$

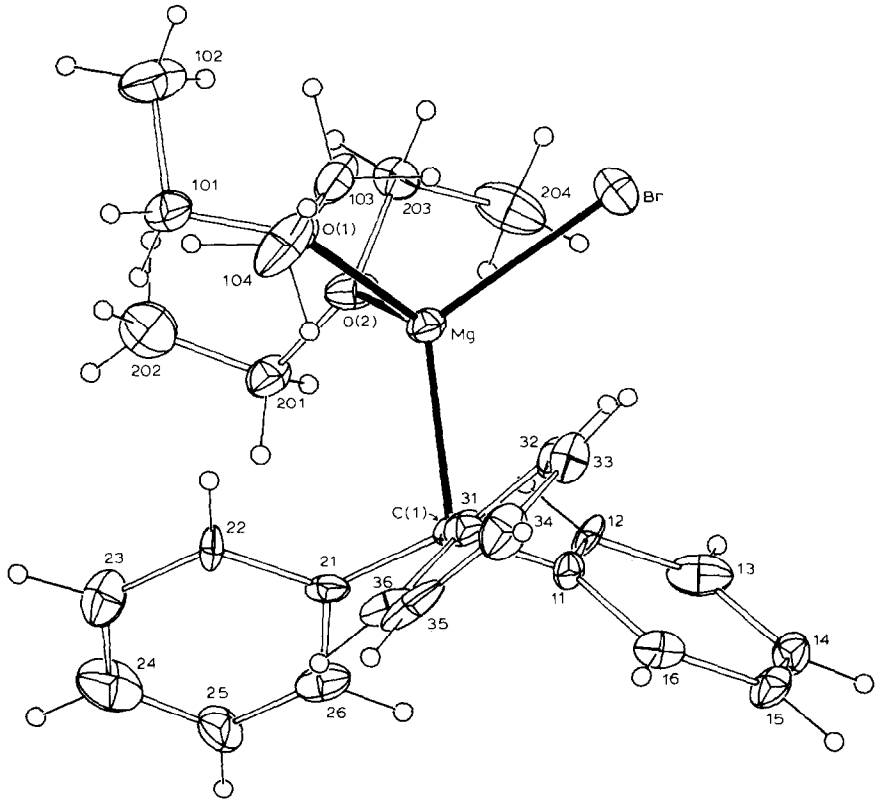

Fig. 2. Molecular structure of $[Mg(CPh_3)Br(OEt_2)_2]$ (**4**) showing 20% thermal ellipsoids for non-hydrogen atoms; hydrogen atoms have radii arbitrarily set at 0.1 Å.

The asymmetric unit in **4** is a single molecule in which the metal centre is a slightly distorted tetrahedron (Fig. 2), as is the norm for diethyl ether adducts of Grignard reagents (viz. $[MgBrR(OEt_2)_2]$, R = Et [26] or Ph [27]). Thus, the steric hindrance of the hydrocarbyl group in **4** is accommodated without change in stoicheiometry or degree of aggregation, the *ipso*-carbon substituents and donor groups on the metal adopting a staggered conformation. Interestingly, the $O(CHMe_2)_2$ adduct of MgBrEt is dimeric with bridging bromine atoms, and only one ether molecule per metal centre [28].

The Mg–C_α distance, 2.25(1) Å cf. $\bar{r}$(Mg–C_β) 2.98 Å is marginally shorter than that in **1**, indicating that more covalency is present in **4**. Unfortunately, we were

Table 1

Non-hydrogen atom coordinates for **1**

Atom	Molecule A			Molecule B		
	x	*y*	*z*	*x*	*y*	*z*
Mg [a]	0	0.79334(9)	0.2206(–)	0.0287(5)	0.5303(1)	0.2324(3)
Anthracene						
C(1)	0.265(1)	0.7743(3)	0.2194(8)	0.314(1)	0.5343(3)	0.2962(8)
C(2)	0.269(1)	0.7940(3)	0.1397(8)	0.307(1)	0.5700(3)	0.2549(8)
C(3)	0.295(2)	0.7805(4)	0.0614(8)	0.357(2)	0.6019(3)	0.2969(8)
C(4)	0.270(2)	0.7999(4)	−0.0100(9)	0.332(2)	0.6341(3)	0.255(1)
C(5)	0.225(2)	0.8349(4)	−0.0081(8)	0.261(2)	0.6336(4)	0.166(1)
C(6)	0.206(2)	0.8504(4)	0.0677(8)	0.217(2)	0.6020(4)	0.1194(9)
C(7)	0.220(1)	0.8306(3)	0.1407(7)	0.241(1)	0.5704(3)	0.1672(7)
C(8)	0.177(1)	0.8427(3)	0.2210(7)	0.181(2)	0.5357(4)	0.1261(9)
C(9)	0.282(1)	0.8286(3)	0.3021(8)	0.288(2)	0.5058(3)	0.1520(9)
C(10)	0.328(2)	0.8481(4)	0.3766(8)	0.323(2)	0.4768(4)	0.103(1)
C(11)	0.410(2)	0.8315(4)	0.4529(8)	0.419(2)	0.4492(4)	0.144(1)
C(12)	0.461(2)	0.7959(4)	0.4521(8)	0.474(2)	0.4469(4)	0.233(1)
C(13)	0.425(2)	0.7783(3)	0.3779(9)	0.455(2)	0.4757(3)	0.278(1)
C(14)	0.333(1)	0.7925(3)	0.3013(8)	0.358(2)	0.5049(3)	0.243(1)
THF 1						
O	−0.1834(9)	0.8044(2)	0.1130(5)	−0.0675(10)	0.5522(2)	0.3312(5)
C(1)	−0.204(2)	0.7828(4)	0.038(1)	0.023(2)	0.5748(4)	0.401(1)
C(2)	−0.251(2)	0.8067(5)	−0.036(1)	−0.064(2)	0.5740(4)	0.470(1)
C(3)	−0.276(2)	0.8419(4)	−0.001(1)	−0.224(2)	0.5535(5)	0.439(1)
C(4)	−0.259(2)	0.8398(4)	0.093(1)	−0.240(2)	0.5465(4)	0.346(1)
THF 2						
O	−0.1095(10)	0.8062(2)	0.3204(5)	−0.0408(10)	0.4800(2)	0.2580(5)
C(1)	−0.051(2)	0.7912(4)	0.4044(9)	−0.064(2)	0.4523(4)	0.194(1)
C(2)	−0.072(2)	0.8199(4)	0.4654(9)	0.015(3)	0.4190(5)	0.240(1)
C(3)	−0.139(2)	0.8516(4)	0.4141(10)	0.057(3)	0.4286(6)	0.323(1)
C(4)	−0.199(2)	0.8396(4)	0.3269(10)	0.011(2)	0.4646(5)	0.341(1)
THF 3						
O	−0.1156(10)	0.7434(2)	0.2216(5)	−0.1990(11)	0.5481(2)	0.1612(5)
C(1)	−0.030(2)	0.7101(4)	0.2214(9)	−0.236(3)	0.5849(5)	0.160(1)
C(2)	−0.168(3)	0.6831(5)	0.232(1)	−0.322(4)	0.5914(7)	0.072(2)
C(3)	−0.330(2)	0.7017(5)	0.219(1)	−0.387(3)	0.5601(6)	0.033(1)
C(4)	−0.302(2)	0.7395(4)	0.2192(9)	−0.300(2)	0.5296(5)	0.090(1)

[a] Mg(A) defines the origin.

Table 2

Non-hydrogen atom coordinates for **4**

Atom	*x*	*y*	*z*
Br	0.14478(9)	0.22007(9)	1/4
Mg	0.2682(3)	0.3086(2)	0.2334(6)
C(1)	0.2529(7)	0.4446(7)	0.2861(12)
C(11)	0.1771(7)	0.4716(8)	0.219(1)
C(12)	0.1646(7)	0.4489(8)	0.090(1)
C(13)	0.0924(11)	0.4752(10)	0.026(2)
C(14)	0.0337(9)	0.5284(9)	0.085(1)
C(15)	0.0471(8)	0.5508(8)	0.209(1)
C(16)	0.1189(8)	0.5249(8)	0.279(1)
C(21)	0.3326(7)	0.4827(7)	0.238(2)
C(22)	0.4069(6)	0.4553(8)	0.277(2)
C(23)	0.4764(9)	0.4879(10)	0.231(2)
C(24)	0.4729(12)	0.5461(11)	0.129(2)
C(25)	0.4021(9)	0.5756(10)	0.083(2)
C(26)	0.3356(10)	0.5452(9)	0.137(2)
C(31)	0.2439(8)	0.4430(8)	0.431(1)
C(32)	0.1875(7)	0.3967(8)	0.495(1)
C(33)	0.1762(9)	0.3974(10)	0.627(2)
C(34)	0.2190(10)	0.4458(11)	0.702(2)
C(35)	0.2777(11)	0.4940(10)	0.651(2)
C(36)	0.2929(10)	0.4950(9)	0.515(2)
O(1)	0.3488(5)	0.2479(6)	0.3495(10)
C(101)	0.4336(10)	0.2314(9)	0.311(2)
C(102)	0.4435(11)	0.1460(9)	0.246(3)
C(103)	0.3256(10)	0.2105(9)	0.474(2)
C(104)	0.3597(12)	0.2543(13)	0.586(2)
O(2)	0.3159(7)	0.2853(5)	0.0530(9)
C(201)	0.3699(8)	0.3415(8)	−0.025(2)
C(202)	0.4470(12)	0.3104(12)	−0.046(2)
C(203)	0.2868(9)	0.2106(9)	−0.016(2)
C(204)	0.2137(13)	0.2310(11)	−0.102(2)

Table 3

Magnesium environments in **1**

Atom	Parameters
Distances (Å)	
Mg–C(1)	2.25(1), 2.31(1)
Mg–C(8)	2.33(1), 2.29(2)
Mg–O(1)	2.059(7), 2.065(10)
Mg–O(2)	2.028(8), 2.029(9)
Mg–O(3)	2.091(8), 2.056(9)
Angles (degrees)	
C(1)–Mg–C(8)	70.9(4), 71.9(5)
C(1)–Mg–O(1)	124.9(4), 97.6(4)
C(1)–Mg–O(2)	130.3(4), 105.2(4)
C(1)–Mg–O(3)	98.1(4), 155.5(4)
C(8)–Mg–O(1)	100.0(3), 150.4(5)
C(8)–Mg–O(2)	100.0(4), 116.2(5)
C(8)–Mg–O(3)	169.0(4), 96.5(5)
O(1)–Mg–O(2)	104.7(3), 93.1(4)
O(1)–Mg–O(3)	86.8(3), 82.0(4)
O(2)–Mg–O(3)	86.5(3), 99.3(4)

Table 4

Molecular core geometry of **4**

Atoms	Parameters
Distances (Å)	
Mg–Br	2.465(5)
Mg–C(1)	2.25(1)
Mg–O(1)	2.02(1)
Mg–O(2)	2.04(1)
C(1)–C(11)	1.48(2)
C(1)–C(21)	1.52(2)
C(1)–C(31)	1.50(2)
Angles (degrees)	
Br–Mg–C(1)	116.4(3)
Br–Mg–O(1)	102.5(3)
Br–Mg–O(2)	105.7(3)
C(1)–Mg–O(1)	113.1(5)
C(1)–Mg–O(2)	115.8(4)
O(1)–Mg–O(2)	101.5(4)
Mg–C(1)–C(11)	105.2(8)
Mg–C(1)–C(21)	102.3(7)
Mg–C(1)–C(31)	103.5(7)
C(11)–C(1)–C(21)	117(1)
C(11)–C(1)–C(31)	113(1)
C(21)–C(1)–C(31)	115(1)

unable to measure the ^{13}C NMR chemical shift of the *ipso*-carbon to corroborate this finding. However, the Mg–C distance in **4** is longer than that in $[MgEtBr(OEt_2)_2]$ (2.15(2) Å) [26]. This most likely arises from more ionic character associated with some delocalization of charge. Consistent with this is the *ipso*-carbon being close to trigonal-planar with respect to the attached carbon atoms ($\Sigma(C–C_{ipso}–C)$ 345°) and that the $Mg–C_{ipso}–C$ angles are markedly less than tetrahedral values (Table 4). Moreover, the mean $C_{ipso}–C$ distances (1.50 Å) are between those of triphenylmethane (1.52_4 Å) [29] and the lithium and sodium contact ion-pair structures (1.46_5 [11] and 1.46_7 Å [12]). The Mg–Br distance, 2.465(5) Å, is within the range established for a variety of four-coordinate monomeric species [26,30]; the Mg–O distances are unexceptional.

Experimental

All operations were carried out under argon using Schlenk and glove-box techniques. Solvents were dried over Na/K (THF) or Na (OEt_2 and benzene) and were freeze-degassed prior to use. Spectroscopic data were obtained on Bruker ER 100 and Hitachi/Perkin–Elmer R-24B EPR and NMR spectrometers, and a Hewlett–Packard 8450A UV/VIS spectrophotometer. Formation of crystals of **1** is described above. All studies of the Grignard reagents derived from $BrCPh_3$ in THF were on freshly prepared solutions since the reagent slowly cleaves THF [33].

Reaction of $BrCPh_3$ with magnesium in THF

To a suspension of magnesium powder (0.18 g, 7.4 mmol) in THF (10 cm^3) was added a few drops of 1,2-dibromoethane. After evolution of ethene had ceased, the

THF was replaced by fresh THF (40 cm^3). $BrCPh_3$ (2.0 g, 6.2 mmol) was then added with stirring at room temperature. The mixture turned yellow, orange than deep red over 1 h. After 12 h, the resulting red precipitate and unreacted magnesium was separated from the mother liquor, and washed with THF (25 cm^3). The resulting filtrate (75 cm^3) had an activity of 2.86×10^{-2} *M* (from acid quenching (0.1 *M* HCl) and back titration with base (0.1 *M* NaOH), which corresponds to 35% yield of solvated Grignard reagent. Quenching with 38% DCl/D_2O gave $DCPh_3$ as the major product.

Reaction of $BrCPh_3$ with [Mg(anthracene)(THF)$_3$] (1) in THF

To an ice-cold slurry of **1** (2.60 g, 6.2 mmol) in THF (40 cm^3) was added $BrCPh_3$ (2.0 g, 6.2 mmol) in THF (20 cm^3) over 30 min. The mixture immediately turned deep red, and a red precipitate formed. This was collected, washed with THF (3×25 cm^3) and dried in vacuo m.p. 82°C (dec), 1.62 g, 45% yield based on the formula $[Mg(CPh_3)Br(THF)_3]$ (a ratio of $[CPh_3]^-$ to THF of 1/3 was established from ^1H NMR studies of the CCl_4 decomposition mixture). The mother liquor (135 cm^3) had an activity of 1.64×10^{-2} *M* which corresponds to 37% yield of solvated Grignard reagent. Quenching with 38% DCl/D_2O gave $DCPh_3$ as the major product.

Reaction of [Mg(CPh$_3$)Br(OEt$_2$)$_2$] (4) with THF

A solution of **4** was prepared from $BrCPh_3$ (2.0 g, 6.2 mmol) in OEt_2 (10 cm^3) and benzene (20 cm^3) according to the literature method [19] (yield 95% from acid quenching and back titration with base), which on dilution gave a ca. 75 line EPR spectrum centred at $g = 2.0031$, matching that reported for $[CPh_3]^{\cdot}$ [23]. Volatiles were removed in vacuo, yielding a light brown solid. Addition of THF (50 cm^3) afforded a dark red solution and a red solid which was collected, washed with THF (25 cm^3) and dried in vacuo (2.0 g, representing a 57% yield based on the formula $[Mg(CPh_3)Br(THF)_3]$ (see above)). The mother liquor had an activity of 2.26×10^{-2} *M* (determined as previously detailed), which corresponds to 28% of solvated Grignard reagent. Quenching with 38% DCl/D_2O gave $DCPh_3$ as the major product.

Structure determination

Unique data sets were measured to the specified $2\theta_{max}$ limit at 295 K using a $P2_1$ four-circle diffractometer in conventional $2\theta/\theta$ scan mode (monochromatic Mo-K_α radiation source, λ 0.7106_9 Å). *N* independent reflections were obtained, N_o with $I > 3\sigma(I)$ being considered "observed" and used in the large block least squares refinement after Gaussian absorption correction and solution of the structure by direct methods. Anisotropic thermal parameters were refined for the non-hydrogen atoms; $(x, y, z, U_{iso})_H$ were constrained at estimated values. Residuals at convergence are conventional *R*, *R'* on $|F|$; statistical weights were used derived from $\sigma^2(I) = \sigma^2(I_{diff}) + 0.0005\ \sigma^4(I_{diff})$. Neutral atom complex scattering factors were used [31]; computation used the XTAL program system [32] implemented by S.R. Hall on a Perkin–Elmer 3241 computer. Results are summarised in Tables 1–4 and Fig. 1 and 2, the latter showing the non-hydrogen atom numbering *.

* Tables of non-hydrogen thermal parameters, hydrogen atom parameters and ligand geometries have been deposited with the Cambridge Crystallographic Centre.

Crystal data. **1**: $C_{26}H_{34}MgO_3$, $M = 418.9$, Monoclinic, space group C_c (C_s^4, No. 9), a 8.039(5), b 37.48(2), c 15.941(6) Å, β 101.94(4)°, U 4700(4) Å^3, D_c 1.18 g cm^{-3} ($Z = 8$). $F(000) = 1808$. μ_{Mo} 1.05 cm^{-1}. Specimen: ~ 0.25 mm (capillary). $2\theta_{max}$ 50°. $N = 4173$, $N_o = 2164$. $R = 0.089$, $R' = 0.091$.

4: $C_{27}H_{35}BrMgO_2$, $M = 495.8$, orthorhombic space group $Pna2_1$ (C_{2v}^9, No. 33), a 16.32(1), b 15.954(9), c 10.253(6) Å, U 2669(3) Å^3, D_c 1.23 g cm^{-3} ($Z = 4$). $F(000) = 1040$. μ_{Mo} 16.8 cm^{-1}. Specimen: 0.40 × 0.40 × 0.52 mm. $A^*_{min,max} = 1.75$, 1.94. $2\theta_{max}$ 45°. $N = 1844$, $N_o = 1225$. $R = 0.062$, $R' = 0.076$. (preferred chirality).

Individual features/variations in procedure were: for **1** the isotropic thermal parameters were refined for the atoms of the tetrahydrofuran moieties. No absorption correction. Data were measured on the reciprocal lattice of a single crystal deconvoluted from a twinned specimen. R is accordingly rather high, probably in consequence of profile overlap and high tetrahydrofuran thermal motion. For **4** the acceptance criterion for "observed" data $2\sigma(I)$ was in order to assist in stabilizing full anisotropic refinement in the context of limited data, high thermal motion, a non-centrosymmetric space group and a heavy atom.

Acknowledgement

We express gratitude for support of this work from the Australian Research Grants Scheme.

References

1 B. Bogdanović, Angew. Chem., Int. Ed. Engl., 24 (1985) 262.
2 J. Scholz and K.-H. Thiele, J. Organomet. Chem., 314 (1986) 7.
3 H. Bönnemann, B. Bogdanović, R. Brinkmann, D-W. He, and B. Spliethoff, Angew. Chem., Int. Ed. Engl., 22 (1983) 728; B. Bogdanović and M. Schwickardi, Z. Naturforsch. B, 39 (1984) 1001.
4 C.L. Raston and G. Salem, J. Chem. Soc., Chem. Commun., (1984) 1702.
5 T. Alonso, S. Harvey, P.C. Junk, C.L. Raston, B.W. Skelton and A.H. White, Organometallics, 6 (1987) 2110.
6 B. Bogdanović, S. Liao, R. Mynott, K. Schlichte, and U. Westeppe, Chem. Ber., 117 (1984) 1378.
7 B. Bogdanović, N. Janke, C. Krüger, R. Mynott, K. Schlichte, and U. Westeppe, Angew. Chem., Int. Ed. Eng., 24 (1985) 960.
8 H. Lehmkuhl, A. Shakoor, K. Mehler, C. Krüger, K. Angermund, and Y.-H. Tsay, Chem. Ber., 118 (1985) 4239.
9 M.F. Lappert, T.R. Martin, C.L. Raston, B.W. Skelton, and A.H. White, J. Chem.Soc., Dalton Trans., (1982) 1959.
10 D.J. Brauer and G.D. Stucky, J. Organomet. Chem., 37 (1972) 217.
11 J.J. Brooks and G.D. Stucky, J. Am. Chem. Soc., 94 (1972) 7333.
12 H. Foster and E. Weiss, J. Organomet. Chem., 168 (1979) 273.
13 M. Gielen, I.V. Eynde, F. Polet, J. Meunier-Piret, and M. Van Meerssche, Bul. Soc. Chim. Belg., 89 (1980) 915.
14 P.C. Junk, C.L. Raston, B.W. Skelton, and A.H. White, J. Chem. Soc., Chem. Commun., (1987) 1162.
15 P.K. Freeman and L.L. Hutchinson, J. Org. Chem., 48 (1983) 879.
16 Y. Kai, N. Kanehisa, K. Miki, N. Kasai, K. Mashima, H. Yasuda, and A. Nakamura, Chem. Lett., (1982) 1277.
17 P.v.R. Schleyer, T. Clark, A.J. Kos, G.W. Spitznagel, C. Rohde, D. Arad, K.N. Houk, N.G. Rondan, and D. Arad, J. Am. Chem. Soc., 106 (1984) 6467; P.v.R. Schleyer, A.J. Kos, D. Wilhelm, T. Clark, G. Boche, G. Decher, H. Etzrodt, H. Dietrich, and W. Mahdi, J. Chem. Soc., Chem. Commun., (1984) 1495.
18 W.E. Rhine, J. Davis, and G. Stucky, J. Am. Chem. Soc., 97 (1975) 2079.

19 M. Gomberg and W.E. Beckmann, J. Am. Chem. Soc., 52 (1930) 2455.
20 H.F. Ebel and B.O. Wagner, Chem. Ber., 104 (1971) 307.
21 E. Buncel and B. Menon, J. Org. Chem., 44 (1979) 317.
22 H.F. Ebel and B.O. Wagner, Chem. Ber., 104 (1971) 320.
23 A. Berndt, H. Fischer, and H. Paul in H. Fischer and K.H. Hellwege (Eds.), Landolt–Bornstein, Magnetic 15 Properties of Free Radicals, Springer-Verlag, Heidelberg, Vol. 9, part b, p. 718.
24 H. Lankamp, W.Th. Nauta, and C. MacLean, Tetrahedron Lett., (1968) 249; J.M. McBride, Tetrahedron, 30 (1974) 2009; N.S. Blom, G. Roelofsen, and J.A. Kanters, Cryst. Struct. Commun., 11 (1982) 297.
25 K.J. Skinner, H.S. Hochster, and J.M. McBride, J. Am. Chem. Soc., 96 (1974) 4301.
26 L.J. Guggenberger and R.E. Rundle, J. Am. Chem. Soc., 90 (1968) 5375.
27 G. Stucky and R.E. Rundle, J. Am. Chem. Soc., 86 (1964) 4825.
28 A.L. Spek, P. Voorbergen, G. Schat, C. Blomberg, and F. Bickelhaupt, J. Organomet. Chem., 77 (1974) 147.
29 C. Riche and C. Pascard-Billy, Acta Crystallog. B, 30 (1974) 1874.
30 H. Kageyama, K. Miki, Y. Kai, N. Kasai, Y. Okamoto, and H. Yuki, Bull. Chem. Soc. Jpn., 57 (1984) 1189.
31 J.A. Ibers and W.C. Hamilton (Eds.), International Tables for X-ray Crystallography, Vol. 4, The Kynoch Press, Birmingham, 1974.
32 J.M. Stewart and S.R. Hall (Eds.). 'The XTAL System of Crystallographic Programs: User's Manual', Technical Report TR-901, Computer Science Center, University of Maryland.
33 F.R. Jensen and R.L. Bedard, J. Org. Chem., 24 (1959) 874.